Seres, J. [et al.] (2018) Non-perturbative generation of DUV/VUV harmonics from crystal surfaces at 108 MHz repetition rate. *Optics express*. Vol. 26, issue 17, p. 21900-21909. DOI: 10.1364/OE.26.021900

Non-perturbative generation of DUV/VUV harmonics from crystal surfaces at 108 MHz repetition rate

J. SERES,[1*] E. SERES,[1] C. SERRAT,[2] T. SCHUMM,[1]

[1] *Atominstitut - E141, Technische Universität Wien, Stadionallee 2, 1020 Vienna, Austria*
[2] *Universitat Politècnica de Catalunya, Departament de Física, Colom 11, 08222 Terrassa, Spain*
**jozsef.seres@tuwien.ac.at*

Abstract: We demonstrate non-perturbative 3rd (267 nm) and 5th (160 nm) harmonic generation in solids from a Ti:sapphire frequency comb (800 nm) at 108 MHz repetition rate. The experiments show that non-perturbative low harmonics are dominantly generated on the surface and on the interface between solids, and that they are not produced by bulk processes from the near-surface layer of the material. Measurements reveal that due to the lack of phase matching, the generated harmonics in bulk are suppressed by orders of magnitude compared to the signal generated on the surface. Our results pave the way for the development of all-solid-state high repetition rate harmonic sources for vacuum ultraviolet spectroscopy and high precision frequency comb metrology.

1. Introduction

High harmonic generation (HHG) is an attractive method to convert ultrashort laser pulses from the infrared or visible spectral range into the vacuum ultraviolet (VUV) or soft x-ray spectral range [1]. It produces a coherent, wide spectrum of several harmonic lines, which makes HHG a widely used method to generate ultrashort probe pulses for time-resolved spectroscopy supporting temporal resolutions in the few-femtosecond and even in the sub-femtosecond time scales and to study ultrafast physical and chemical processes. For a long time, harmonics have been generated in different gases, and HHG from solids has attracted attention only in recent years, after the first successful demonstrations of the phenomenon [2, 3] using mid-infrared laser pulses and later THz driving fields [4].

In solids, harmonics can be generated at much lower laser intensities than in gases, promising the extension of HHG into very compact laser sources and with very high repetition rates, reaching even GHz frequencies. Such high repetition rates would be very beneficial for time-resolved spectroscopic applications, and VUV or EUV frequency combs [5-7] could also be realized in solids for high precision metrology. Consequently, HHG in solids is being extensively explored both experimentally and theoretically. Experiments using low repetition rate laser sources as pump have demonstrated HHG in different bulk crystals [8-11] and 2D materials [12-14] and the first high repetition rate generation at 70-80 MHz has recently been reported in sapphire [15-17]. Based on dynamical Bloch oscillations [4, 18], non-perturbative generation of HHG in solids is usually explained by interband and intraband transitions of the electrons inside the band-structure of solids as they interact with the incident laser field as bulk processes [10, 11, 19]. In some cases, the generation of harmonics is also described as perturbative cascaded three-wave [20] or four-wave mixing [21] processes.

Several recent studies have suggested the need to further investigate the precise generation of harmonics in solids in order to accurately differentiate between bulk and surface generation, and between perturbative and non-perturbative processes. Indeed, in [15] the generation of harmonics in solids was observed only from the near-surface layer in sapphire, in the 60-120 nm spectral range, and this effect was explained by considering the strong absorption of sapphire, which enables only the last about 10-nm-thick layer of the crystal to contribute to the HHG signal. Other experiments have found that the 3rd harmonic of a fiber

laser at 531 nm is also generated only near the crystal surfaces, at a wavelength where the crystal is however basically transparent [16]. Additionally, high harmonics have been successfully generated in single layer materials [12-14] and efficient generation of the 3rd harmonic at around 700 nm from a single layer graphene has been reported [22].

In this work, we show that low order harmonics (3rd and 5th) generated by strong-field driven nonlinear processes in solids are predominantly generated on the surface or on the interface between solids, and that they cannot be correctly described as non-phase-matched perturbative or non-perturbative bulk processes. In our measurements, instead of changing the laser intensity itself, which would give a similar dependence of the harmonics signal for generation on the surface and the bulk, we apply a z-scan technique that allows accurately distinguishing between bulk and surface processes. We first study different fluoride crystals that are transparent at both 3rd and 5th harmonic wavelengths of the 800-nm Ti:sapphire frequency comb. We show that the experimental results are consistent with non-perturbative generation of harmonics on the solid surface and cannot be explained as perturbative bulk harmonics. We then investigate GaN films on a sapphire substrate, which strongly absorbs at both the 3rd and 5th harmonics, in order to differentiate between non-perturbative bulk and surface processes. Our measurements show that non-phase matched harmonics from bulk are orders of magnitude weaker than those from the surface.

2. Experimental setup

The experimental setup is shown in Fig. 1(a). A Ti:sapphire frequency comb (FC8004, Menlo Systems) delivered linearly polarized pulses at 800 nm with a pulse duration of 20 fs and a pulse energy of 8 nJ at 108 MHz repetition rate. The pulses were negatively chirped by chirp-mirror pairs for pre-compensation of the dispersion in air, the wedge-pair used for dispersion fine tuning and the dispersion of the focusing lens. About 7 nJ of the laser pulses reached the sample crystals. A lens with focal length of 10 mm was applied to focus the laser beam onto the crystal. The beam waist in the focus was 5.5±0.5 µm, resulting in a peak intensity of ~1x10^{12} W/cm^2 and a Rayleigh length of 120±20 µm.

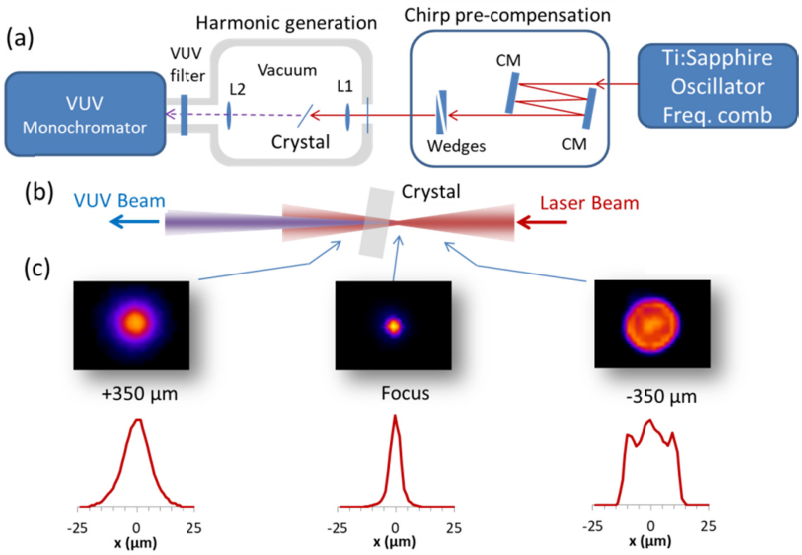

Fig. 1. Experimental setup. (a) CM: chirped mirror; L1: BK7 lens, f = 10 mm; L2: MgF_2 lens, f = 40 mm. (b) Magnified area around the crystal. (c) The beam profiles of the focused laser beam before, at, and after the focus measured by replacing the crystal with a CCD camera.

The samples were tilted by about 10°, see Fig. 1(b), to avoid back-reflection into the frequency comb. The generated harmonic beam was focused with a VUV-grade MgF_2 lens to the input slit of a VUV monochromator (McPherson 234/302) equipped with a 300 l/mm grating. According to earlier measurements [15], the harmonic beams co-propagate with the fundamental laser beam, with any small deviations corrected by the lens that collects them onto the spectrometer slit. The HHG sample and the VUV monochromator were in vacuum with a background pressure of 10^{-3} mbar. In certain measurements, a VUV bandpass filter was inserted into the HHG beam at the entrance of the monochromator to suppress the 3rd harmonic. The spectrally resolved beam was detected with a VUV photomultiplier (Hamamatsu R6836), sensitive in the 115-320 nm spectral range, which prevented us from detecting the 7th or higher harmonic orders which would also be present.

3. Harmonic generation on fluoride crystals

In the first measurement series, fluoride crystals, namely LiF, MgF_2, and CaF_2 were used with different thicknesses. They are commercially available with optically polished VUV windows at crystal orientations of (100), (110) and (111). These crystals are wide bandgap isolators with absorption edges in the 120-140 nm range. Beyond being transparent in the VUV, these fluoride crystals have small non-linear refractive indexes in the range of $1\text{-}2\times10^{16}$ cm^2/W [23], which gives a non-linear phase shift in the order of $\pi/100$ causing negligible non-linear spectral or beam profile distortion during propagation in the crystals. Otherwise, our conclusions below are drawn mainly from measurements performed when the focus is before the crystal surface, in vacuum, as shown in Fig. 1(b). The samples were mounted in a motorized rotation stage with the rotation axis perpendicular to the surface, which allows finding the direction of the strongest harmonic signal. Furthermore, the crystals were translated along the optical axis of the laser beam through the focal region (z-scan).

Figure 2(a) shows the measured spectra from the crystals optimally positioned and rotated to get the highest signal. As it will be seen later in Fig. 3, harmonics (especially the 5th one) are stronger from the back surface. The VUV filter was not used here to be able to measure the weak 5th harmonic from LiF, and consequently, the 3rd harmonics saturated the detector. In the case of CaF_2, the signal would reach about 5-times higher. As it can be seen from Fig. 2, from all fluoride crystals almost the same strong 3rd harmonic can be generated. The difference however is large in the case of the 5th harmonic. A suitably strong 5th harmonic is produced in CaF_2 and a weaker signal is obtained in LiF, while from MgF_2 it was not possible to generate 5th harmonic.

Moving the CaF_2 crystal along the optical axis away from the optimum position, the laser intensity on the surface is scanned in a wide intensity range and the intensity of the generated 3rd and 5th harmonics is measured and plotted in Fig. 2(b). Here we measured the generated harmonics on the front surface, because it was possible to change the laser intensity in a wider range without the interference from the other surface. In the experiments, the laser beam was focused but still with a NA<0.1 so that the paraxial approximation is preserved. To determine the laser intensity on the surface, a focused beam with a certain divergence θ is assumed. The laser intensity depends on the beam radius $w(z)$ as $I(z) \propto w^{-2}(z)$ and the beam radius can be approximated by a quadratic form as $w^2(z) \approx a_0 + a_1 z + \theta^2 z^2$, giving $w(z) \approx \theta z$ at large z values. The laser intensity can be written as

$$I(z) \propto \left\{ \theta^2 z_R^2 \left[1 + \left(z - z_0 \right)^2 / z_R^2 \right] \right\}^{-1}, \tag{1}$$

where z_0 is the position of the beam waist, z_R is the Rayleigh length, and $z = 0$ or $z = L$ at the back or at the front surface of the crystal, respectively, with L being the crystal thickness. The intensity of the fundamental laser beam is therefore calculated using Eq. (1) and gives the

horizontal axis of Fig. 2(b). As it is well visible in Fig. 2(b), the intensity dependence of the harmonic q can be accurately described with a power function

$$I_q \propto I_{surface}^{q'}. \tag{2}$$

According to earlier results obtained in gas harmonics [24], for non-perturbative harmonics, q' is not determined and can be obtained by fitting the theory to the measurements, while for perturbative bulk harmonics $q'=q$-1 [25], meaning $q'=2$ and $q'=4$ for the 3rd and the 5th harmonics, respectively. It is clear from the slope of the curves in Fig. 2(b), which gives 4.3 for the 3rd and 3.2 for the 5th harmonic, that the generation of the harmonics was produced in a non-perturbative manner.

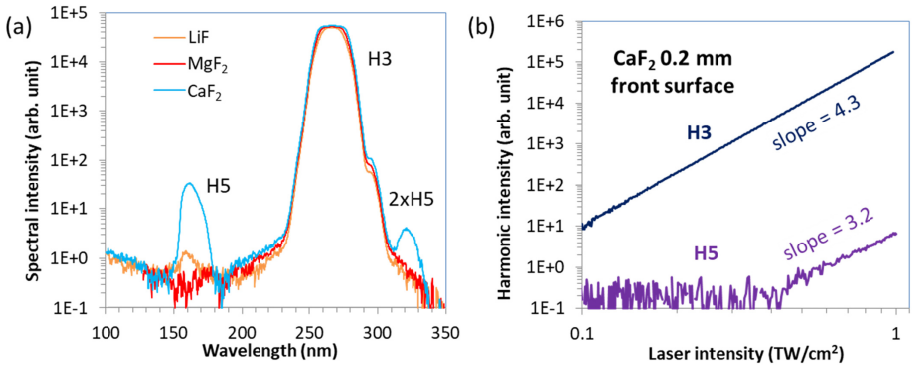

Fig. 2. (a) Measured spectra of 3rd and 5th harmonics from different fluoride crystals, generated on the back surface of the crystals at laser intensity of 1 TW/cm^2. (b) Measured harmonic intensity generated on the front surface depends on the laser intensity on the surface what dependence can be well approximate with a power function.

4. Z-scan measurement on the fluoride crystals

To examine the generation of harmonics in more detail, a z-scan was performed by translating the crystals along the optical axis of the laser beam through the focal region and the intensity of the generated 3rd harmonic, in every case, and the intensity of the 5th harmonic, in the case of CaF_2, was measured with the VUV monochromator. The obtained curves are plotted in Fig. 3.

Every measured curve shows a strongly pronounced double-peak structure with one peak at the zero positions ($z = 0$, when the laser focus coincides with the back surface) and another one at the position corresponding to the front surface of the crystal, which depends on the crystal thickness ($z = L$). When the focus was inside the crystal, the intensity of the generated harmonics was always much reduced, fact that has also been observed earlier [16, 21]. We observe an oscillating structure on the left slope of the curves [see Fig. 3(a) and 3(c)], that is independent of the crystal material and thickness, which is related to the shape of the laser beam before the focus [see Fig. 1(c)]. Indeed, in the focus and after it the measured beam profiles were smooth and nearly Gaussian, yielding a smooth right slope of the curves. To fit the calculations to the measured curves, we use

$$I_q(z_0) = c_0 \left[1 + \left(L - z_0\right)^2 / z_R^2\right]^{-q'}, \tag{3}$$

which is derived from Eq. (1) and Eq. (2).

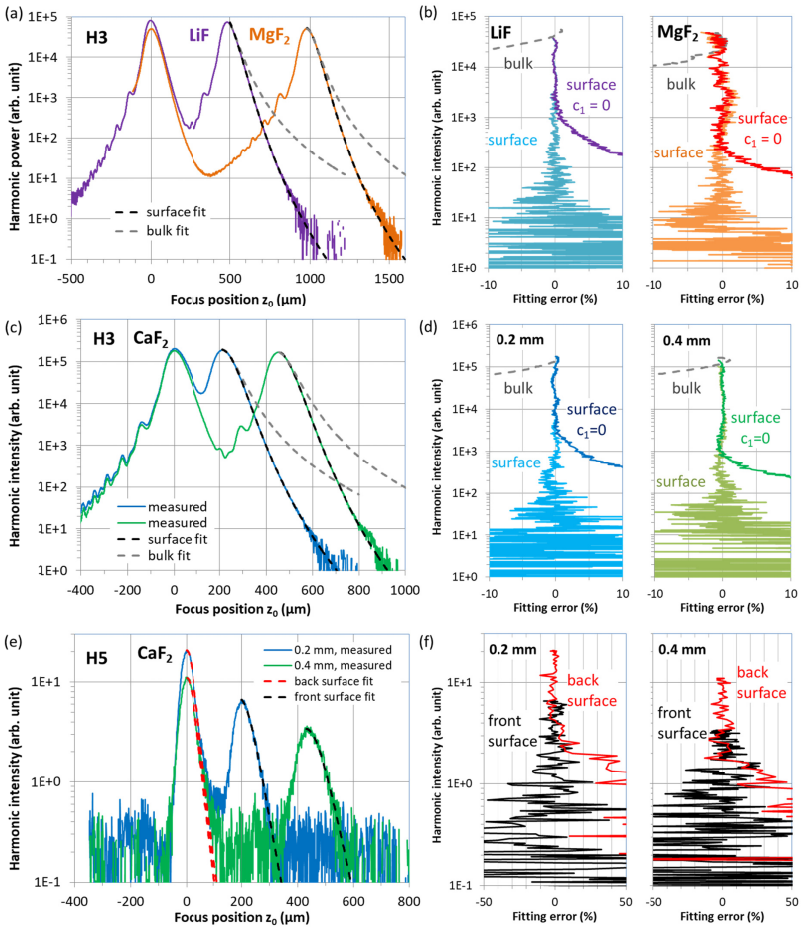

Fig. 3: Z-scan for fluoride crystals. Measured focus position dependent intensity of the generated 3rd harmonic from (a) LiF 0.5 mm (violet) and MgF_2 1.0 mm (red) crystals and the generated (c) 3rd harmonic and (e) 5th harmonic from CaF_2 crystals with a thickness of 0.2 mm (blue) and 0.45 mm (green),. The calculated harmonic intensities are plotted with dashed black and red curves assuming surface harmonics, and with dashed gray curves assuming bulk harmonics. The panels at the right side (b,d,f) show the calculated fitting errors for the cases.

In Figs. 3(a) and 3(c), we first perform a fit by assuming bulk generation of the 3rd harmonic with q'=2, using c_0 and z_R as fitting parameters, and in Figs. 3(b) and 3(d) we show the calculated fitting errors for the front surface of the crystals. These results are plotted with dashed gray curves in Figs. 3(a)-3(d). It is clear that the calculations assuming perturbative bulk harmonics divert quickly from the measurements. Next, we perform a second fit by adding q' as fitting parameter and the fitting errors are plotted in Figs. 3(b) and 3(d) with dark colored curves (violet, red, blue and green). Contrarily to the fit obtained by assuming bulk generation, surface harmonics with $q' \approx 4.4 \pm 0.3$ and $z_R \approx 135 \pm 10$ μm fit very well (< 1 %) over an intensity range of 2-orders of magnitude at the large harmonic intensities, and divert only at the low intensities. This divergence is an artefact due to some background signal from the scattered fundamental laser light, which we can remove from the measured signal by using

$$I_q(z_0) = I_{q,meas}(z_0) - c_1\left[1 + (z_1 - z_0)^2 / z_{R1}^2\right]^{-1}. \qquad (4)$$

The measured curves in Fig. 3(a) and 3(c) are plotted after this background correction. As it can be seen in Figs. 3(a)-3(d), i.e. after background correction of the measured signal, the calculated curves fit very well, over 3-4 orders of magnitude of the intensity range, and the fit is only limited by the measurement noise at the very low intensities. The corrected background has a very small contribution to the signal with c_0/c_1 in the range of 3000-6000. Table 1 summarizes all the used fitting parameters. The data in Table 1 shows that the background should originate from the back surface of the crystal, because the focus position (z_1) is shifted. Such a small contribution cannot be observed from the front surface, because it is within the fitting error.

Table 1. Fitting parameters

		LiF	MgF_2	CaF_2 H3		CaF_2 H5	
crystal parameters	L (mm)	0.5	1	0.2	0.45	0.2	0.45
	n	1.39	1.38	1.43			
fitting parameters	L (μm)	449	970	208	443	190	430
	z_R (μm)	146	128	124	137	106	123
	q'	4.6	4.09	4.29	4.67	3.8	3.5
	z_1 (μm)	704	1250	432	699		
	z_{R1} (μm)	106	106	98	87		
	c_0/c_1	5700	5700	3800	4900		

Because of the weaker signal of the 5th harmonic, see Fig. 3(e), it was not possible to perform measurements with a similar dynamic range as in the case of the 3rd harmonic, but it is still possible to fit Eq. (3), and no background correction is necessary. We get a good fit with $q' \approx 3.6 \pm 0.2$, which is indeed different from the bulk case ($q'=4$). The fit was limited only by the measurement noise in the case of the front surface or by the added contribution of the other surface in the case of the back surface, as it can be seen in Fig. 3(f). We can conclude from this analysis that assuming non-perturbative harmonics generated on the crystal surface accurately describes the measurements over several orders of magnitude of the intensity range.

5. Z-scan measurement on the GaN layer on sapphire

In a second measurement series, a GaN layer (a wurtzite crystal structure with thickness of 5 μm) on a sapphire substrate (thickness of 430 μm) having (0001) orientation was used. In these measurements we make use of the fact that GaN is a semiconductor with a bandgap of 3.4 eV and consequently strongly absorbs both the 3rd and the 5th harmonic of a Ti:sapphire laser, while the sapphire substrate is transparent at both harmonic wavelengths [26]. The sample was again moved along the optical axis of the laser beam through the focal region (z-scan) and the intensity of the generated 3rd or 5th harmonic were measured with the VUV monochromator. The results are plotted in Fig. 4(a). The measurements were performed when the GaN layer was on the back surface (light/dark-blue lines); on the front surface (orange line) of the substrate; and also with a sapphire sample without GaN layer (thickness of 500 μm, black dashed line) for comparison. As it can be seen in Fig. 4(a), the 3rd harmonic generated from the GaN layer was up to 2000 times stronger than that from the sapphire sample without the GaN layer. It was only possible to generate 5th harmonic from the GaN layer (not from the sapphire). The measured spectra from the GaN layer and from a substrate without layer are shown in Fig. 4(b). The spectra of the 5th harmonic are also shown separately in Fig. 4(c) with linear scale.

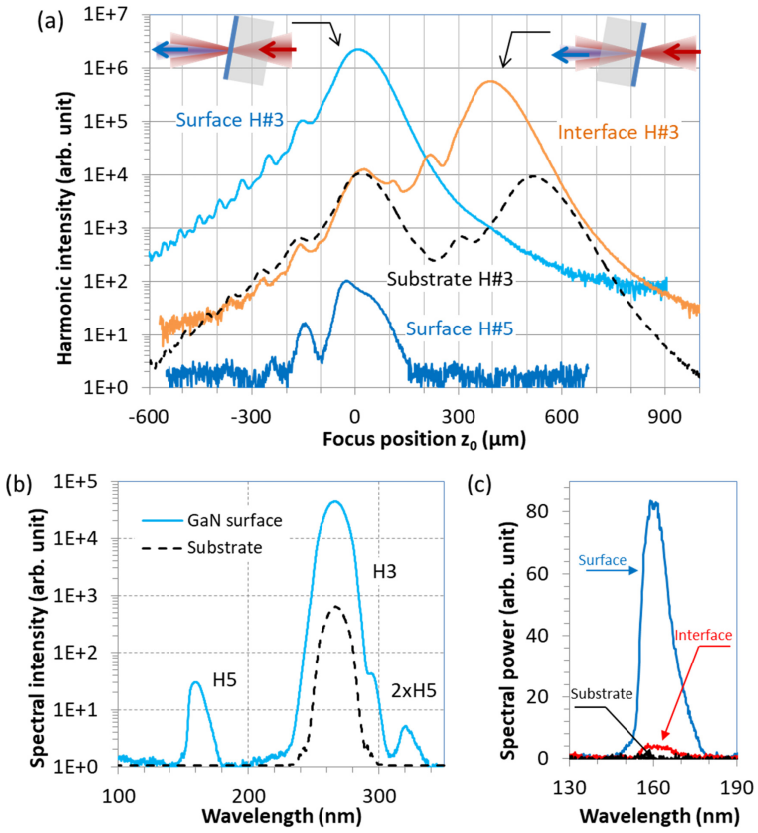

Fig. 4: GaN on sapphire. (a) Generated 3rd and 5th harmonic signals from a thin GaN layer (5-µm-thick) on a sapphire substrate (430-µm-thick) as the focus position moves through the crystal (z-scan). The black dashed line shows the 3rd harmonic generated from a sapphire sample (~500-µm-thick) without GaN layer. The insets show the relative position of the focused laser beam with respect to the sample in two cases when maximum signals were generated. (b) Measured harmonic spectra of the sample consisting of a GaN layer and of the sapphire substrate alone both at $z_0=0$ focus position. (c) Measured spectra of 5th harmonic generated on the GaN surface [blue, upper-left inset in (a)], the GaN-sapphire interface [red, upper-right inset in (a)] and on the substrate back surface (black).

In these measurements, if one expected the generation of harmonics within the GaN layer as bulk harmonics, the measured signals should have been independent of whether the layer was situated on the front or on the back surface. This is because the sapphire substrate is transparent at both harmonic wavelengths, and the conditions of the harmonic generation are very similar for the GaN layer at both surfaces. The generated 3rd harmonic from the substrate alone was also roughly symmetric from both surfaces [similarly to the fluoride crystals, see the dashed-black line in Fig. 4(a)]. The present measurements however exhibit a very different behavior. Indeed, the 3rd harmonic signal can reach an about 4-times higher value, noted by the black arrows in Fig. 4(a), when the GaN layer is on the back surface. In the case of the 5th harmonic, this ratio even reached about 20 [see Fig. 4(c)]. This behavior is consistent only if we assume that the harmonics are mainly generated at the surfaces and the interfaces between solids, and not in the bulk material. Certainly, in this configuration, we have three surfaces, one is the GaN–vacuum interface, the second is the GaN–sapphire interface, and the third is the sapphire–vacuum interface. These interfaces are

morphologically different and one can expect a difference in the harmonic generation efficiency. The obtained results can therefore be explained as follows:

- Black dashed line (Substrate H3): when a sapphire sample was used without any GaN layer, the 3rd harmonic signal peaked at the two positions where the focus is at the surfaces. The harmonic signals from the two surfaces were about the same, as expected, because the two surfaces were equivalent. The 5th harmonic was not generated by the sapphire without a GaN layer.

- Light/dark blue lines (Surface H3/H5): when the GaN layer was on the back surface of the sapphire substrate, a strong 3rd harmonic signal and a weaker 5th harmonic were clearly generated from the back surface of the GaN layer (GaN–vacuum interface). These harmonic signals decreased as the laser intensity decreased on the surface, as the focus was moved away from the surface. They were generated at the GaN–vacuum interface because the harmonic signals generated at the GaN–sapphire interface and at the sapphire-vacuum interface (sapphire front surface) were absorbed by the GaN layer.

- Orange line (Interface H3): the GaN layer was on the front surface. At zero focus position (sapphire–vacuum interface) a weak 3rd harmonic signal was generated, the same as from the sapphire crystal alone, as it would be expected. At the focus position of 430 μm, when the GaN layer was in the focus, a strong 3rd harmonic signal was generated, but about 4-times weaker than in the case that the layer was on the back surface (light blue curve). This harmonic signal did not originate from the front surface of the GaN layer (GaN–vacuum interface), because that signal was absorbed by the GaN layer. Furthermore, the harmonic signal could not be generated inside the bulk GaN layer, as if this were the case it would have shown the same signal strength as in the case where the GaN layer was on the back surface (light blue curve). The harmonic signal was hence generated on the GaN–sapphire interface. The 5th harmonic signal was too weak to be measured in a z-scan and only the spectrum (at the focus position on GaN) was measured [see Fig. 4(c)].

6. Conclusion

In conclusion, we generated intense 3rd harmonic from different fluoride crystals, 5th harmonic from CaF_2 crystals, and 3rd and 5th harmonics from a crystalline GaN layer on a sapphire substrate. We showed experimentally that these harmonics were generated from the surfaces or the interfaces between the crystals in a non-perturbative manner. We find no contribution from perturbative bulk harmonics in the measured signals, meaning that for the 3rd harmonic non-perturbative surface contribution should be 4-5 orders of magnitude larger.

Further studies are needed to examine the high efficiency of the harmonics generated from the surface, and few new studies already started to address this question. In [27] it is theoretically shown that from topological edge states, harmonics can be 14-orders of magnitude more efficiently generated than from bulk, what may be applicable to surfaces. An experimental study [28] reports that from the interface between two materials the second harmonic can be more efficiently generated. High harmonics on a surface in reflection geometry have also been generated [29].

Based on our findings, suitably nano-engineered surfaces may greatly improve the efficiency of non-perturbative harmonic generation [30-33]. Designed multilayer structures based on surface harmonics can also improve harmonic generation efficiency by means of quasi-phase matching.

Funding

European Union's Horizon 2020 (664732); Wiener Wissenschafts- und Technologie Fonds (WWTF) (MA16-066 “SEQUEX”); Spanish Ministry of Economy and Competitiveness through “Plan Nacional” (FIS2017-85526-R).

Acknowledgment

The authors thank Erin Young for providing samples that triggered and helped this line of research.

References

1. M. C. Kohler, T. Pfeifer, K. Z. Hatsagortsyan, and C. H. Keitel, "Frontiers of Atomic High-Harmonic Generation," Adv. Atom. Mol. Opt. Phys. **61**, 159-207 (2012).
2. A. H. Chin, O. G. Calderon, and J. Kono, "Extreme Midinfrared Nonlinear Optics in Semiconductors," Phys. Rev. Lett. **86**, 3292-3295 (2001).
3. S. Ghimire, A. D. DiChiara, E. Sistrunk, P. Agostini, L. F. DiMauro, and D. A. Reis, "Observation of high-order harmonic generation in a bulk crystal," Nat. Phys. **7**, 138-141 (2011).
4. O. Schubert, M. Hohenleutner, F. Langer, B. Urbanek, C. Lange, U. Huttner, D. Golde, T. Meier, M. Kira, S. W. Koch and R. Huber, "Sub-cycle control of terahertz high-harmonic generation by dynamical Bloch oscillations," Nat. Phot. **8**, 119-123 (2014).
5. C. Gohle, T. Udem, M. Herrmann, J. Rauschenberger, R. Holzwarth, H. A. Schuessler, F. Krausz, T. W. Hansch, "A frequency comb in the extreme ultraviolet," Nature **436**, 234-237 (2005).
6. A. Cingoz, D. C. Yost, T. K. Allison, A. Ruehl, M. E. Fermann, I. Hartl, and J. Ye, "Direct frequency comb spectroscopy in the extreme ultraviolet," Nature **482**, 68-71 (2012).
7. G. Winkler, J. Fellinger, J. Seres, E. Seres, and T. Schumm, "Non-planar femtosecond enhancement cavity for VUV frequency comb applications," Opt. Express **24**, 5253-5262 (2016).
8. T. T. Luu, M. Garg, S. Y. Kruchinin, A. Moulet, M. T. Hassan, and E. Goulielmakis, "Extreme ultraviolet high-harmonic spectroscopy of solids," Nature **521**, 498-502 (2015).
9. G. Ndabashimiye, S. Ghimire, M. Wu, D. A. Browne, K. J. Schafer, M. B. Gaarde, and D. A. Reis, "Solid-state harmonics beyond the atomic limit," Nature **534**, 520-523 (2016).
10. A. A. Lanin, E. A. Stepanov, A. B. Fedotov, and A. M. Zheltikov, "Mapping the electron band structure by intraband high-harmonic generation in solids," Optica **4**, 516-519 (2017).
11. Y. S. You, M. Wu, Y. Yin, A. Chew, X. Ren, S. Gholam-Mirzaei, D. A. Browne, M. Chini, Z. Chang, K. J. Schafer, M. B. Gaarde, and H. Ghimire, "Laser waveform control of extreme ultraviolet high harmonics from solids," Opt. Lett. **42**, 1816-1819 (2017).
12. N. Yoshikawa, T. Tamaya, K. Tanaka, "High-harmonic generation in graphene enhanced by elliptically polarized light excitation," Science **356**, 736-738 (2017).
13. H. Liu, Y. Li, Y. S. You, S. Ghimire, T. F. Heinz, and D. A. Reis, "High-harmonic generation from an atomically thin semiconductor," Nat. Phys. **13**, 262-265 (2017).
14. M. Taucer, T. J. Hammond, P. B. Corkum, G. Vampa, C. Couture, N. Thire, B. E. Schmidt, F. Legare, H. Selvi, N. Unsuree, B. Hamilton, T. J. Echtermeyer, and M. A. Denecke, "Nonperturbative harmonic generation in graphene from intense midinfrared pulsed light," Phys. Rev B **96**, 195420 (2017).
15. H. Kim, S. Han, Y. W. Kim, S. Kim, and S.-W. Kim, "Generation of Coherent Extreme-Ultraviolet Radiation from Bulk Sapphire Crystal," ACS Photonics **4**, 1627-1632 (2017).
16. G. Yi, H. Y. Lee, J. Jiannan, B. J. Chun, S. Han, H. Kim, Y. W. Kim, D. Kim, S.-W. Kim, and Y.-J. Kim, "Nonlinear third harmonic generation at crystalline sapphires," Opt. Express **25**, 26002-26010 (2017).
17. Kevin F. Lee, Xiaoyan Ding, T. J. Hammond, M. E. Fermann, G. Vampa, and P. B. Corkum, " Harmonic generation in solids with direct fiber laser pumping," Opt. Lett. **42**(6), 1113-1116 (2017).
18. T. Dekorsy, R. Ott, and H. Kurz, "Bloch oscillations at room temperature," Phys. Rev. B **51**, 17275-17278 (1995).
19. T. T. Luu, and H. J. Worner, "High-order harmonic generation in solids: A unifying approach," Phys. Rev. B **94**, 115164 (2016).
20. D. D. Hickstein, D. R. Carlson, A. Kowligy, M. Kirchner, S. R. Domingue, N. Nader, H. Timmers, A. Lind, G. G. Ycas, M. M. Murnane, H. C. Kapteyn, S. B. Papp, and S. A. Diddams, "High-harmonic generation in periodically poled waveguides," Optica **4**, 1538-1544 (2017).
21. N. Garejev, I. Grazuleviciute, D. Majus, G. Tamosauskas, V. Jukna, A. Couairon, and A. Dubietis, "Third- and fifth-harmonic generation in transparent solids with few-optical-cycle midinfrared pulses," Phys. Rev. A **89**, 033846 (2014).
22. C. Beckerleg, T. J. Constant, I. Zeimpekis, S. M. Hornett, C. Craig, D. W. Hewak, and E. Hendry, "Cavity enhanced third harmonic generation in graphene," Appl. Phys. Lett. **112**, 011102 (2018).
23. D. Milam, M. J. Weber, and A. J. Glass, "Nonlinear refractive index of fluoride crystals," Appl. Phys. Lett. **31**, 822 (1977).
24. L. A. Lompre, A. L'Huillier, M. Ferray, P. Monot, G. Mainfray, and C. Manus, "High-order harmonic generation in xenon: intensity and propagation effects," J. Opt. Soc. Am. B **7**, 754-761 (1990).
25. R. W. Boyd, "Nonlinear Optics," Academic Press, Inc. ISBN 0-12-121680-2 (1992).
26. E. R. Dobrovinskaya, L. A. Lytvynov, and V. Pishchik, "Sapphire: Material, Manufacturing, Applications," ISBN 978-0-387-85695-7, Springer Science + Business Media, LLC (2009).
27. D. Bauer, and K. K. Hansen, "High-Harmonic Generation in Solids with and without Topological Edge States," Phys. Rev. Lett. **120**, 177401 (2018).

28. X. Zhao, Y. Zheng, N. An, H. Ren, X. Deng, and X. Chen, "Enhancement of UV Second-Harmonic Radiation at Nonlinear Interfaces with Discontinuous Second-order Susceptibilities," Sci. Rep. **8**, 6695 (2018).
29. G. Vampa, Y. S. You, H. Liu, S. Ghimire, and D. A. Reis, "Observation of backward high-harmonic emission from solids," Opt. Express **26**(9), 12210-12218 (2018).
30. D. Golde, T. Meier, and S. W. Koch, "High harmonics generated in semiconductor nanostructures by the coupled dynamics of optical inter- and intraband excitations," Phys. Rev. B **77**, 075330 (2008).
31. G. Vampa, B. G. Ghamsari, S. S. Mousavi, T. J. Hammond, A. Olivieri, E. Lisicka-Skrek, A. Y. Naumov, D. M. Villeneuve, A. Staudte, P. Berini, and P. B. Corkum, "Plasmon-enhanced high-harmonic generation from silicon," Nat. Phys. **13**, 659-662 (2017).
32. M. Sivis, M. Taucer, G. Vampa, K. Johnston, A. Staudte, A. Y. Naumov, D. M. Villeneuve, C. Ropers, P. B. Corkum, "Tailored semiconductors for high-harmonic optoelectronics," Science **357**, 303-306 (2017).
33. L. Shi, J. R. C. Andrade, H. Kim, S. Han, R. Nicolas, D. Franz, W. Boutu, T. Heidenblut, F. B. Segerink, B. Bastiaens, H. Merdji, S.-W. Kim, U. Morgner, and M. Kovacev, "Investigating the origin of third harmonic generation from diabolo optical antennas," Appl. Phys. Lett. **111**, 173102 (2017).